Journal Name

ARTICLE TYPE

Cite this: DOI: 00.0000/xxxxxxxxxx

Electronic Supplementary Information for "Room Temperature Second Sound in Cumulene"

Claudio Melis,*[a] Giorgia Fugallo,[b] and Luciano Colombo[a]

1 Description of the model potential used for the calculations.

All the classical MD simulations have been performed by using the LAMMPS code[1] and a Class II force field[2] that has been specifically adapted to reproduce the cumulene phonon dispersion curves calculated at Density Functional Theory (DFT) level. The functional form of the present force field is the following:

$$E_{total} = E_b + E_\theta + E_{b,b'} + E_{vdW} \tag{1}$$

where

$$\begin{aligned} E_b &= \sum_b k_{b1}(b-b_{eq})^2 + k_{b2}(b-b_{eq})^3 + k_{b3}(b-b_{eq})^4 \\ E_\theta &= \sum_\theta k_{\theta 1}(\theta-\theta_{eq})^2 + k_{\theta 2}(\theta-\theta_{eq})^3 + k_{\theta 3}(\theta-\theta_{eq})^4 \\ E_{b,b'} &= \sum_{b,b'} k_{b,b'}(b-b_{eq})(b'-b'_{eq}) \\ E_{vdW} &= \sum_{i<j} 4\varepsilon_{ij}\left[\left(\frac{\sigma_{ij}}{r_{ij}}\right)^{12} - \left(\frac{\sigma_{ij}}{r_{ij}}\right)^{6}\right] \end{aligned} \tag{2}$$

The functional form is divided in two type of interactions: valence terms (E_b, E_θ, $E_{b,b'}$); and nonbonding interaction terms (E_{vdW}). The valence terms describe internal coordinates of bonds (b) and angles (θ), while the cross-coupling term ($E_{b,b'}$) describes the combinations of two internal coordinates. The cross-coupling terms are crucial for properly describe vibrational frequencies, moreover, in particular their inclusion in the functional form allows to describe the occurrence of the Kohn anomaly in the phonon dispersion curves. In Eq. 2 the subscript "eq" denotes the reference values of the bonds and angles, while k_{b1}, k_{b2}, k_{b3}, $k_{\theta 1}$, $k_{\theta 2}$, $k_{\theta 3}$, and $k_{b,b'}$ are the force constants. All the parameters (see Table 1) have been specifically estimated for cumulene by fitting the phonon dispersion curves calculated at Density Functional Theory (DFT) level.

[a] Department of Physics, University of Cagliari, Cittadella Universitaria, I-09042 Monserrato (CA), Italy; E-mail: claudio.melis@dsf.unica.it
[b] LTeN, UMR 6607 CNRS PolytechNantes, Université de Nantes, 44306 Nantes, France

2 Density functional theory calculations.

DFT calculations have been performed using the Quantum-Espresso package[3] and the GGA-PBE exchange-correlation functional[4]. The primitive unit cell of cumulene, consisting of one carbon atom, has been fully relaxed to obtain the equilibrium lattice constant of 1.282 Å. We used an electronic wave-vector grid of 1×1×300 for the Brillouin zone integration with a Marzari-Vanderbilt smearing[5] in the electronic occupations of 0.02 Ry, and a vacuum of 20 a.u. between cumulene chains. The value of the plane-wave energy cutoff was set to 90 Ry. Electron-ion interactions were modelled using a projector augmented wave PAW pseudopotentials[6]. The phonon dispersion curves have been calculated by means of Density Functional Perturbation Theory (DFPT)[7], as implemented in the Quantum-Espresso package using a q-point grid of 1×1×96. The phonon dispersion curves shown in Fig.1 of the main text are in agreement with those of Ref. 8.

3 Thermomechanical effects

In addition to the "second-sound" peak observed in the Fourier transform $F^A(\omega)$ of the time dependent amplitude (shown in Fig.4 of the main text), it is as well found another peak at higher frequency (see Fig.2). We attribute this peak to a thermomechanical effect: a sinusoidal thermal stress is generated along the chain by the initial sinusoidal temperature profile[9]. Similarly to the situation found in graphite and discussed in Ref. 10 this thermal stress excites the chain into a high frequency vibrational mode making the atoms vibrate along the chain, in turns this leads to an oscillatory contribution in $A(t)$. As due to the relatively lower time-resolution (3.5 GHz in Ref. 11 vs. 100 GHz in our simulations), the occurrence of this second peak could not be experimentally observed in graphite. In order to further investigate the nature of this high frequency peak in Fig.1, using the same procedure described in the main text to estimate v_{ss}, we predict its propagation velocity to be as large as 42 Km/s in agreement with the sound velocity of 36 Km/s estimated from the phonon group velocities. This result confirms the thermomechanical nature of the high frequencies peaks observed in the Fourier transform of the amplitude decays.

Table 1 Parameters occurring in the the valence and van der Waals terms of the Class II model potential of Eq. 2

E_b	b_{eq} (Å)	k_{b1} (Kcal mol^{-1} Å^{-2})	k_{b2} (Kcal mol^{-1} Å^{-3})	k_{b3} (Kcal mol^{-1} Å^{-4})
	1.228	2500.0	210.0	1147.0
E_θ	θ_{eq} (radian)	$k_{\theta 1}$ (Kcal mol^{-1} radian^{-2})	$k_{\theta 2}$ (Kcal mol^{-1} radian^{-3})	k_{θ_3} (Kcal mol^{-1} radian^{-4})
	2π	11.3	30.0	40.0
$E_{b,b'}$	b_{eq} (Å)	b'$_{eq}$ (Å)	$k_{b,b'}$ (Kcal mol^{-1} Å^{-1})	
	1.255	1.255	2500	
E_{vdW}	ε_{CC} (Kcal mol^{-1})	σ_{CC} (Å)		
	0.25	3.685		

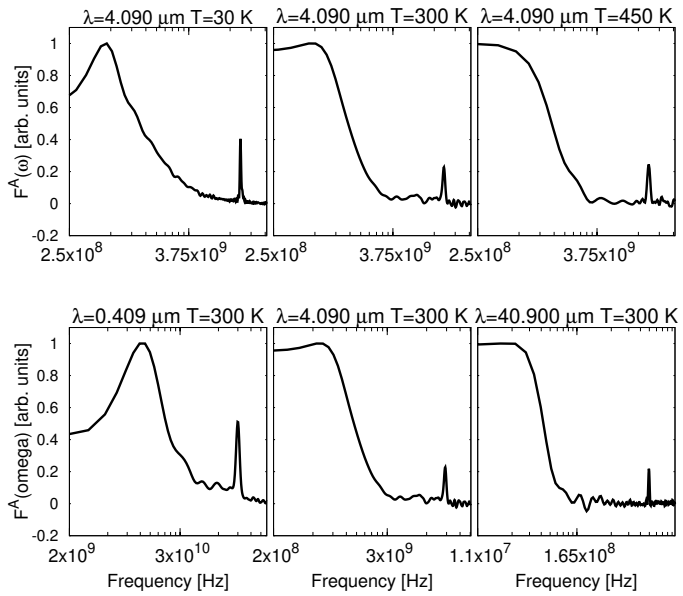

Fig. 1 Top: Fourier transform of the amplitude $A(t)$ for temperatures T=30, 300 and 450 K (top) and spatial periods λ=0.404, 4.090 and 40.900 μm (bottom).

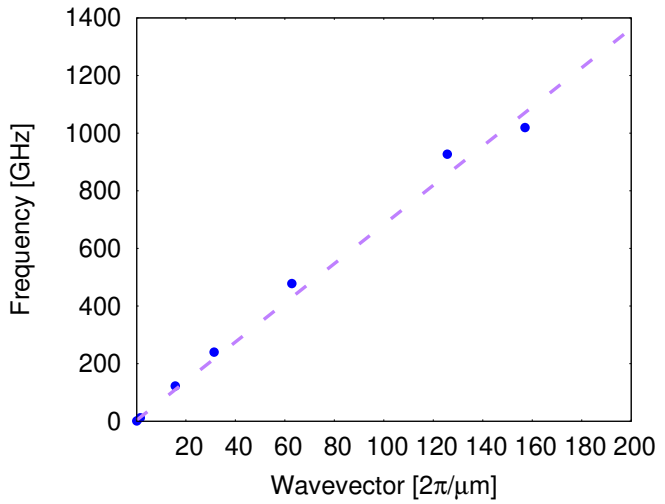

Fig. 2 Blue circles: estimated first-sound frequency as a function of the wave vector. The purple dashed lines represents the corresponding linear fitting function.

3.1 Thermal conductivity of cumulene

For sufficiently large λ values, where an overall diffusive thermal transport regime is observed, we estimate the cumulene thermal diffusivity α at T=300 K by fitting the exponential decay of $A(t)$ with the approximate solution of the 1D heat diffusion equation. In this case the time constant is $\tau_{diff} = \lambda^2/4\pi^2\alpha$, where λ is the spatial period and α is the thermal diffusivity. The thermal conductivity κ is then obtained as $\kappa = \alpha c_v \rho$, where c_v is the specific heat and ρ the mass density. The specific heat c_v has been estimated using the classical expression of Dulong-Petit. The system volume has been estimated by multiplying the cumulene chain length L_x times its cross-sectional area of 3.35 Å$\times$ 3.35 Å as in Ref. 12. Fig.3 shows the calculated thermal conductivity as a function of the spatial period λ. At variance with other 1D systems for which an anomalous divergent thermal conductivity ($\kappa \sim \lambda^\beta$ where β is predicted to fall in between 0.4 and 0.5) was observed [13,14], our simulations (red squares) predict a rather different trend with respect to the one expected for anomalous transport (black and blue full lines, and shaded light-blue area), showing that thermal transport in a cumulene chain is in fact diffusive. Previous works [12] considered an interatomic potential able to reproduce the phonon frequencies only at the Brillouin Zone center, but missing completely the correct phonon- dispersion at the zone boundary. This modeling of phonon dispersions misguided the Authors of Ref. 12 to the incorrect prevision of a largely extended ballistic regime. With the previous force field of Ref. 12 phonons at the border zone never approach one to each other and, therefore Umklapp processes are unphysically reduced. On the contrary, phonon dispersions are well represented by our novel force field as well as Normal/Umklapp processes and their changing relative rates. As a consequence, the higher the temperature (and so the larger the phonon population at the border zone) the more the Umklapp process will be activated. From Fig.3 it is therefore possible to estimate the thermal conductivity value κ_{bulk} as large 20.0$\pm$3.4 KWm^{-1}K^{-1} (instead of the 200 KWm^{-1}K^{-1} suggested in Ref. 12).

3.2 Estimated v_{ss} and τ_{ss} values by means of the MCV equation.

As described in the main text (see Fig.2), we fitted the amplitude decay $A(t)$ with the approximate solution of the Maxwell-Cattaneo-Vernotte (MCV) equation by assuming the same space and time conditions as in our MD simulations i.e. an initial sinusoidal temperature profile and periodic boundary conditions in

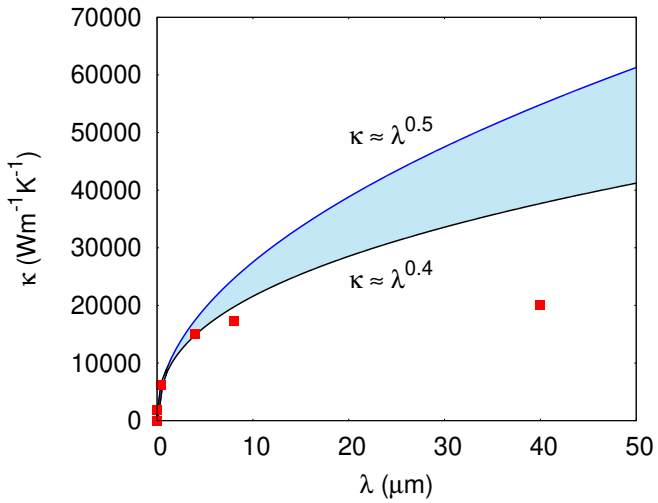

Fig. 3 Thermal conductivity as a function of the spatial period λ for a cumulene chain (red squares) . The shaded area represents the range of typical anomalous thermal transport.

Table 2 Estimated v_{ss} and τ_{ss} values obtained by fitting the $A(t)$ time-decay with the approximate solution of the Maxwell-Cattaneo-Vernotte equation for different temperatures and spatial period λ=4.090 μm.

λ (μm)	T (K)	$v_{ss}(Km/s)$	τ_{ss} (ps)
4.090	30	2.47±0.18	75.87±11
4.090	300	3.23±0.23	138.37 ±23

space: $A(t) \sim \exp(-t/2\tau_{ss})\cos(qv_{ss}t)$, where τ_{ss} is the thermal relaxation time, $q = 2\pi/\lambda$ is the wavevector and v_{ss} is the second sound velocity. We observe a general good agreement between the MCV fitting curve and the corresponding $A(t)$ decay obtained from molecular dynamics. Tables 2 and 3 show the v_{ss} and τ_{ss} values obtained by the fitting procedure for different spatial periods and temperatures.

Table 2 shows the v_{ss} and τ_{ss} values at fixed spatial period λ=4.090 μm for the two limiting temperatures (T=30, 300) of the hydrodynamic regime. We observe a general v_{ss} increase with temperature as previously predicted for graphene[15,16]. Interestingly, the v_{ss} value obtained at T=30 K is in very good agreement with the corresponding value (2.680±0.055 Km/s) obtained by linearly fitting the $\omega = \omega(q)$ dependence (see Fig.5 in the main text). τ_{ss} shows as well a general increase with temperature in the hydrodynamic regime as previously shown for graphene[17]. Table 3 shows the v_{ss} and τ_{ss} values obtained for different spatial periods (λ=0.404 and 4.090 μm) and fixed temperatures T=30 and 300 K. v_{ss} is only marginally affected by the spatial period while τ_{ss} shows a remarkable increase

Table 3 Estimated v_{ss} and τ_{ss} values obtained by fitting the $A(t)$ time-decay with the approximate solution of the Maxwell-Cattaneo-Vernotte equation for different spatial periods and T=30 and 300 K.

λ (μm)	T (K)	$v_{ss}(Km/s)$	τ_{ss} (ps)
0.404	30	2.74 ±0.31	14.2±8
4.090	30	2.47±0.18	75.87±11
0.404	300	3.54 ±0.43	18.2±9
4.090	300	3.23±0.23	138.37±23

Notes and references

1 S. Plimpton, *Fast parallel algorithms for short-range molecular dynamics*, Sandia national labs., albuquerque, nm (united states) technical report, 1993.

2 J. R. Maple, M.-J. Hwang, T. P. Stockfisch, U. Dinur, M. Waldman, C. S. Ewig and A. T. Hagler, *Journal of Computational Chemistry*, 1994, **15**, 162–182.

3 P. Giannozzi, O. Andreussi, T. Brumme, O. Bunau, M. B. Nardelli, M. Calandra, R. Car, C. Cavazzoni, D. Ceresoli, M. Cococcioni *et al.*, *Journal of Physics: Condensed Matter*, 2017, **29**, 465901.

4 J. P. Perdew, K. Burke and M. Ernzerhof, *Physical review letters*, 1996, **77**, 3865.

5 N. Marzari, D. Vanderbilt, A. De Vita and M. Payne, *Physical review letters*, 1999, **82**, 3296.

6 P. E. Blöchl, *Physical review B*, 1994, **50**, 17953.

7 P. Giannozzi, S. De Gironcoli, P. Pavone and S. Baroni, *Physical Review B*, 1991, **43**, 7231.

8 N. Rivano, *MSc thesis*, University of Cagliari, 2018.

9 D. Tsai and R. MacDonald, *Physical Review B*, 1976, **14**, 4714.

10 B. C. Daly, H. J. Maris, K. Imamura and S. Tamura, *Physical review B*, 2002, **66**, 024301.

11 S. Huberman, R. A. Duncan, K. Chen, B. Song, V. Chiloyan, Z. Ding, A. A. Maznev, G. Chen and K. A. Nelson, *Science*, 2019, **364**, 375–379.

12 M. Wang and S. Lin, *Scientific reports*, 2015, **5**, 18122.

13 A. Crnjar, C. Melis and L. Colombo, *Physical Review Materials*, 2018, **2**, 015603.

14 S. Lepri, R. Livi and A. Politi, *EPL (Europhysics Letters)*, 1998, **43**, 271.

15 P. Scuracchio, K. Michel and F. Peeters, *Physical Review B*, 2019, **99**, 144303.

16 S. Lee, D. Broido, K. Esfarjani and G. Chen, *Nature communications*, 2015, **6**, 6290.

17 A. Cepellotti, G. Fugallo, L. Paulatto, M. Lazzeri, F. Mauri and N. Marzari, *Nature communications*, 2015, **6**, 1–7.